

Femtosecond Laser Materials Processing

*P. S. Banks, B. C. Stuart, A. M. Komashko, M. D. Feit, A.
M. Rubenchik, and M. D. Perry*

This article was submitted to
Photonics West 2000 Symposium, San Jose, CA,
January 23-28, 2000

March 6, 2000

U.S. Department of Energy

Lawrence
Livermore
National
Laboratory

DISCLAIMER

This document was prepared as an account of work sponsored by an agency of the United States Government. Neither the United States Government nor the University of California nor any of their employees, makes any warranty, express or implied, or assumes any legal liability or responsibility for the accuracy, completeness, or usefulness of any information, apparatus, product, or process disclosed, or represents that its use would not infringe privately owned rights. Reference herein to any specific commercial product, process, or service by trade name, trademark, manufacturer, or otherwise, does not necessarily constitute or imply its endorsement, recommendation, or favoring by the United States Government or the University of California. The views and opinions of authors expressed herein do not necessarily state or reflect those of the United States Government or the University of California, and shall not be used for advertising or product endorsement purposes.

This is a preprint of a paper intended for publication in a journal or proceedings. Since changes may be made before publication, this preprint is made available with the understanding that it will not be cited or reproduced without the permission of the author.

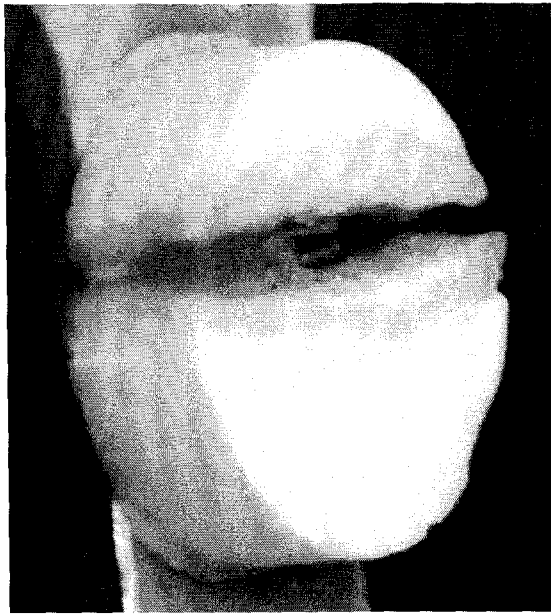
This report has been reproduced
directly from the best available copy.

Available to DOE and DOE contractors from the
Office of Scientific and Technical Information
P.O. Box 62, Oak Ridge, TN 37831
Prices available from (423) 576-8401
<http://apollo.osti.gov/bridge/>

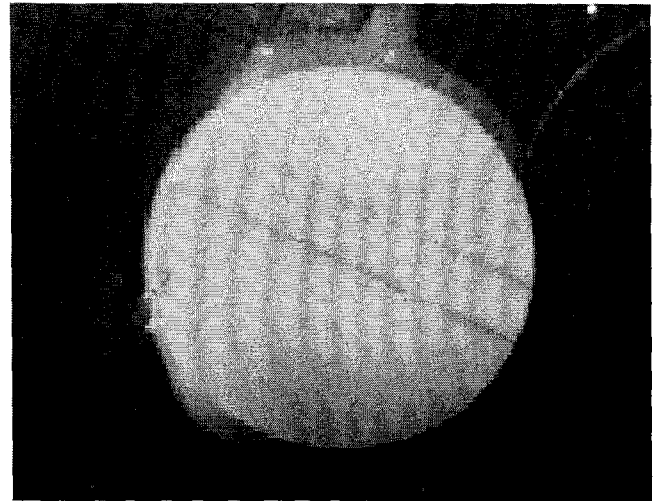
Available to the public from the
National Technical Information Service
U.S. Department of Commerce
5285 Port Royal Rd.,
Springfield, VA 22161
<http://www.ntis.gov/>

OR

Lawrence Livermore National Laboratory
Technical Information Department's Digital Library
<http://www.llnl.gov/tid/Library.html>



(a)



(b)

Fig.1. 2 mm thick LX-16 (PETN) pellet cut by (a) 500 ps pulses and by (b) 150 fs pulses.

In contrast, femtosecond laser pulses deposit their energy in an optical skin depth (typically tens of nanometers thick), creating a region of very high energy density. This occurs even in transparent materials as multi-photon absorption or tunnel ionization can create the free electrons necessary for absorption of remainder of the light pulse.⁸ The material in this thin disk, a solid density plasma, quickly expands away from the surface before a significant amount of the deposited energy can be transferred to the bulk of the material. Although the details of the interaction are different for dielectric materials and metals, the overlying results are the same. Also, because of the nature of the energy deposition process, laser characteristics such as laser wavelength play a much less important role, and it is possible to successfully precision-machine nearly any material.

The main disadvantage of using ultrafast lasers is the need to have high repetition rate/high average power because less than one micron of material is typically removed per pulse. Depending on the feature size required and the throughput requirements, laser systems need to be from a few hundred milliwatts to tens of watts in average power with pulse repetition rates greater than 1 kHz. Ultrafast lasers in this class tend to be highly complex, but short pulse laser technology is steadily progressing. Commercial systems that can produce several watts are now available, and they are becoming increasingly turn-key. At LLNL, we have produced a 15 W system running at 10 kHz with a computerized control system to be used in a production environment by non-laser personnel. In the future, advances in ultrafast laser technology will enable smaller, more reliable systems which can achieve the necessary throughput for industrial applications.

One striking example of how the nonthermal ablation mechanism of femtosecond lasers can be of benefit is the machining of high explosives. Explosives are particularly sensitive to heat and shock and provide an excellent test of our theoretical understanding of this process. Two 6 mm diameter, 2 mm thick samples of LX-16 explosive were cut using a 1 kHz Ti:sapphire laser at 825 nm; one with the pulse uncompressed at 500 ps, and the other with the pulse compressed to 150 fs. The resulting cuts are shown in Fig. 1. The cut done with the 500 ps pulse (Fig. 1(a)) caused ignition of the explosive material, resulting in a sonic burn and poor cut quality. In contrast, the cut done with 150 fs pulses (Fig. 1(b)) resulted in excellent quality slots approximately 25–50 μm wide through 2 mm of material. FTIR analysis on the walls of the slots shows no evidence of reaction products so that the walls are equivalent to unmachined material. We have also been able to drill 100 μm holes through 1 cm of explosive material at a rate of 3–5 μm /pulse, again with no evidence of initiating the chemical reaction. However, increasing the pulse length to 3 ps increased the hole size by a factor of 10 with evidence of burning, and the hole depth was limited to less than 2 mm.

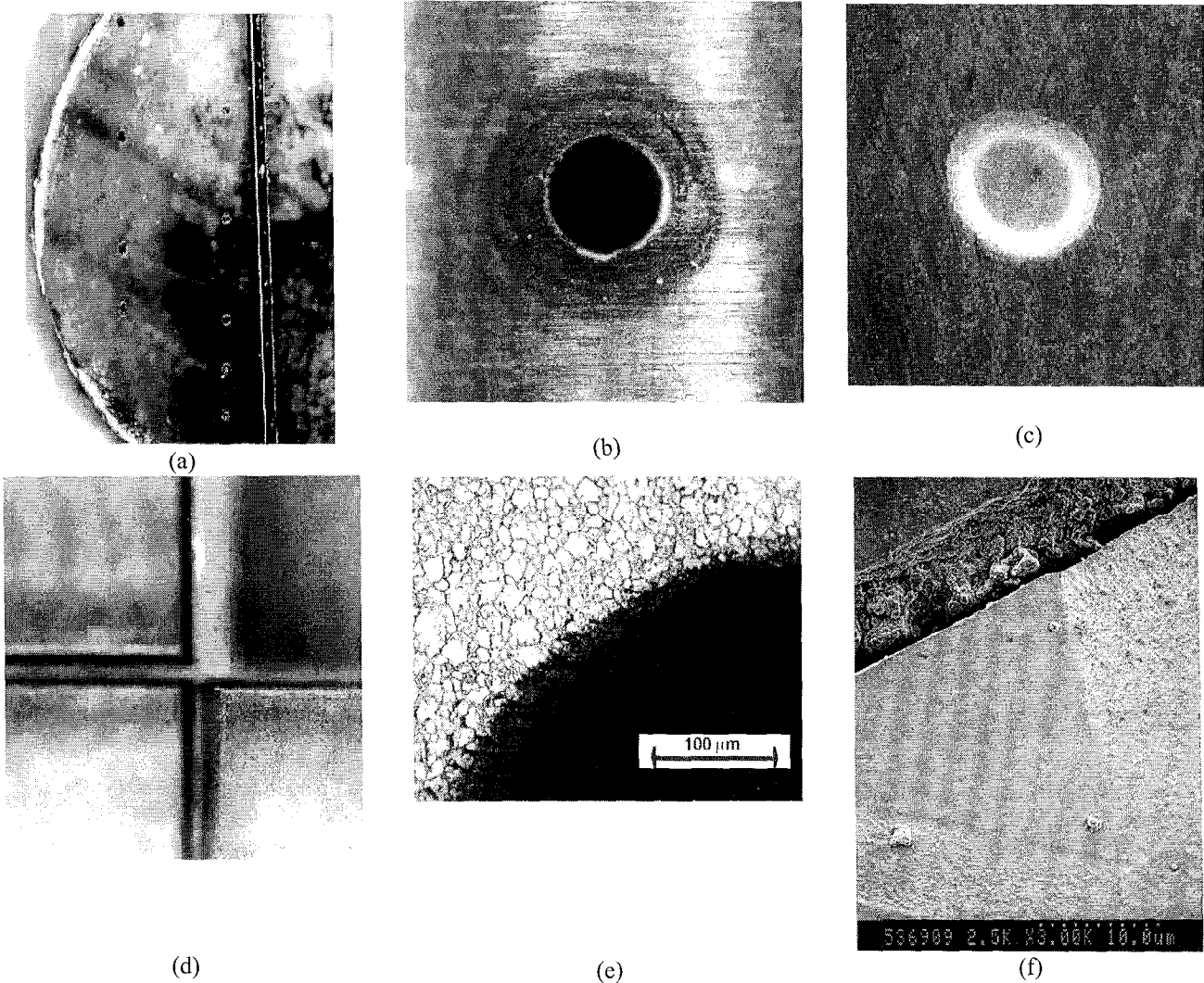
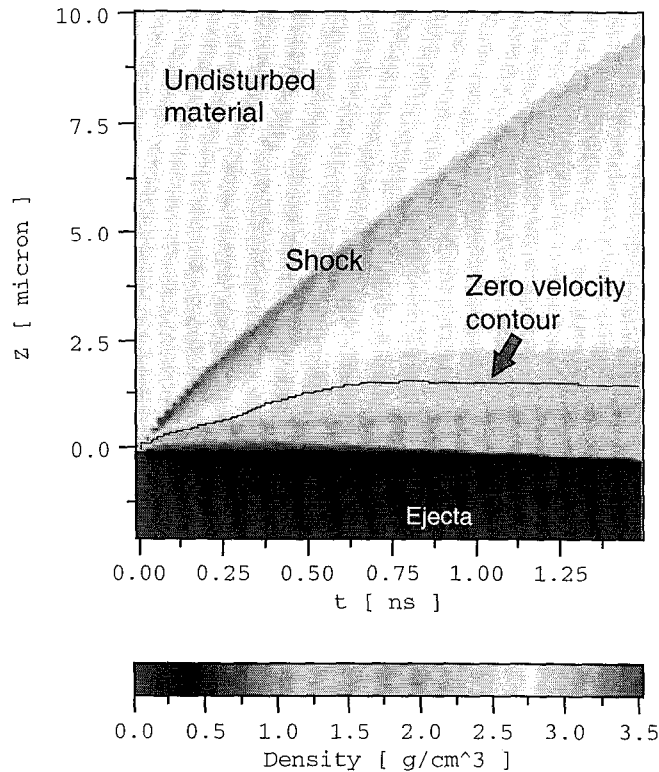


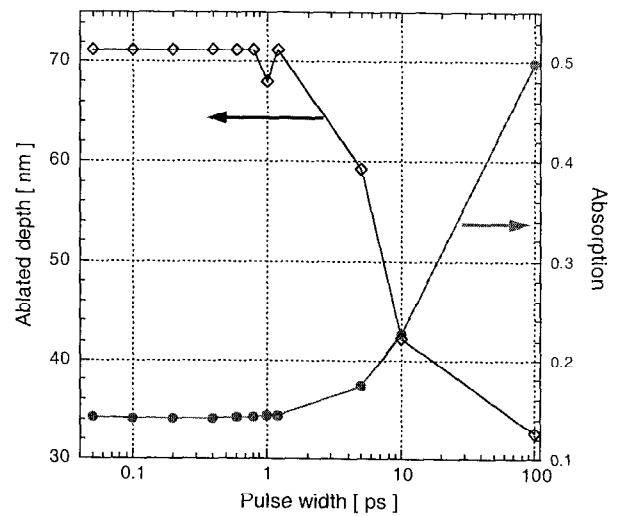
Fig. 2. (a) 50 μm holes and 50 μm slot in diamond wafer. (b) 500 μm holes in SiN. (c) 200 μm hole in tooth. (d) 80 μm slots in polymer. (e) Edge of 500 μm hole in stainless steel. (f) SEM micrograph of cross-section of hole in stainless steel.

Although the machining of high explosives is a rather esoteric application of femtosecond laser machining, it illustrates in dramatic fashion the advantages that can be obtained. We have used femtosecond lasers to drill and cut a wide variety of material with equally good results. Examples of these are diamond, silicon nitride, human teeth, polymers, and many types of metals. Photographs of the features machined in these materials are shown in Fig. 2 along with a high magnification micrograph of the wall of a hole drilled in stainless steel after being cross-sectioned. There is no evidence of any kind of recast or remelt layer, and the grain boundaries are undisturbed up to the wall of the hole. This was done without using trepanning or other post-processing technique to clean up the wall surface. In addition to the materials shown in Fig. 2, we have processed cornea, muscle, bone, sapphire, SiC, Si, Au, Be, Cu, Ti, Al, Ta, W, alloys, all DOD/DOE high explosives, and various composites with equal success.

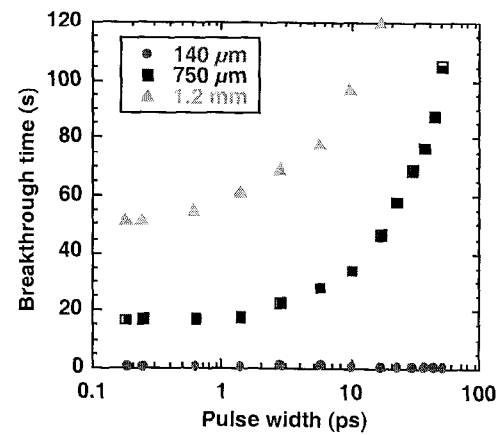
Finally, in addition to the increased quality in the features machined using short pulse lasers, it is also possible to make use of the plasma plume for diagnostics as well as for thin film deposition. The spectroscopic content of the plasma plume can be used as a diagnostic to identify the material being ablated and detect when there is a transition in the material being ablated. An example of when this capability would be useful is for laser-drilling holes in a vertebra. It is necessary to detect when the laser reaches the nerve bundle to avoid unwanted damage. The spectroscopic signatures of bone and the tissue surrounding the nerve are quite different so when the change is detected, the laser beam can be rapidly turned off. Here, the fact that only a small amount is ablated per pulse becomes an advantage and makes it easy to avoid damage to the nerve.⁹



(a)



(b)



(c)

Fig. 3. Calculation of depth of removed material during one pulse. (a) shows the mass density as a function of distance from interface and time with the zero-velocity contour shown as black line. (b) shows corresponding removal depth per pulse as a function of pulse length. (c) shows experimental measurement of breakthrough time as a function of pulse length for 140 μm , 750 μm , and 1200 μm thick material

Because short pulse lasers produce a hot, highly-ionized plasma that subsequently expands in a well-defined fashion, it also can serve as an excellent source for the deposition of thin films. The plasma plume does not exhibit the same splatter and droplet content that is often the case with long-pulse laser-produced plasmas, enabling the production of films which are free from particulates without the need for buffer gases or other mechanisms to remove such particulates. The high intensities also make it easy to produce plumes with large concentrations of ionic species with high kinetic energies (> 100 eV); this has been shown to be important for the production of high quality diamond-like carbon films.¹⁰ We have grown carbon films which have a tetrahedral (sp^3) bond ratio of up to 50%, but of particular importance is that we have been able to grow films of up to 18 μm in thickness.¹¹ Most PLD films must be annealed to achieve thicknesses of more than a few hundred nanometers because of high internal stresses. The fact that we can produce film 100X thicker with no special processing indicates that the internal stresses are different for short pulse PLD. Using 3 W average power at 1 kHz repetition rate, we were also able to achieve growth rates of up to 26 $\mu\text{m}/\text{hr}$ although because the plasma plume is highly directed, we are only able to grow films 1–2 cm in diameter.

3. MODELING

In order to increase our understanding of the underlying ablation process, we have developed a computer model based on a radiation-hydrodynamic computer code named Hyades.^{12,13} This code allows the calculation of the absorption of the incident laser energy in various material zones as a function of electron density, laser polarization and incident angle. Because the depth of the interaction region is small—on the order of the optical skin depth—compared to the transverse extent of the laser beam, the one-dimensional nature of this code should be sufficient. However, this precludes accounting for any effect of transverse variations in either the material or the incident laser light. It also does not allow for analysis of the effect of the walls once a hole or slot has been formed.

One quantity of interest is the ablation rate, particularly as it relates to the incident laser pulse length. Our model does not account for phase change or internal material strength nor does it account for any redeposition mechanisms. It is therefore difficult to assess what material is removed using this type of model. Nonetheless, we are able to calculate the velocities of the material as a function of position and time so we can use the zero-velocity contour as a first estimate of the boundary between the material that is removed and that which remains. This is illustrated in Fig. 3(a) which shows the calculated density vs. position and time for aluminum at 45° angle of incidence, 20 J/cm², 200 fs, and P polarization. The depth of the zero-velocity contour reaches a steady-state value after approximately 500 ps so it is plausible that this contour would be related to the depth at which material leaves the surface and is removed. The dependence on the incident pulse length of the calculated depth removed for one pulse is shown in Fig. 3(b) for 2 J/cm² normally incident in aluminum. The ablation rate is essentially independent of pulse length below 1 ps, above which the rate decreases dramatically. This is because more of the laser energy is absorbed in the plasma plume too far from the original surface to play a roll in ablation—Fig. 3(b) also shows the calculated increase in absorption (the dots) as the pulse length increases above 1 ps. We were able to qualitatively verify this behavior experimentally by measuring the time to breakthrough for several thicknesses of stainless steel as shown in Fig. 3(c) (other metals, including aluminum, show similar behavior). The time to breakthrough is relatively independent of pulse length for pulse lengths less than approximately 1 ps. This indicates that the ablation depth per pulse (obtained by dividing the sample thickness by the number of pulses) is independent of pulse length for pulses shorter than 1 ps in agreement with the calculation shown in Fig. 3(b). Also, the times shown in Fig. 3(c), as is typical, indicate that there is a reduction in the ablation rate in thicker samples.

4. RATES

The experimentally measured rates shown in Fig. 3(c) were determined by measuring the amount of time required for light to be first detected through the exit surface of the workpiece and then dividing the thickness by the total number of pulses required. This is typically how rates reported in the literature are measured. However, the evolution of a hole is complicated and the method used to measure the rate affects the value obtained. Fig. 4 shows an SEM photomicrograph of a blind hole drilled in stainless steel along with a crude depiction of how this hole would look in cross-section. There are two main features: there is the larger hole with an ostensibly flat bottom and there is a smaller, central hole (which we'll refer to as a channel) approximately 40 μm in diameter which extends deeper into the material. There are also smaller “channels” surrounding the main one, but they do not extend as deep into the workpiece so we will limit the discussion at present to the main channel. These channels are characterized by a nearly perfect circular shape and have smooth walls. As will be discussed below, each of these features propagates into the bulk material at a different rate, with the ablation rate of the channel being what is measured by using breakthrough detection. Another possible rate of interest would be the volume of material removed per pulse, but this is difficult to determine because of the irregularities that develop as seen in the hole shown in Fig. 4. It should also be noted that the rate measured can be dependent on depth or shot number (as mentioned above for Fig. 3(c)).¹⁴⁻¹⁵

The average rate at which these features propagate into the workpiece is shown in Fig. 5 as a function of fluence for normal incidence in three materials: stainless steel, aluminum, and copper. The pulse length used in this case is 1 ps to lessen nonlinear effects in the vacuum window and final focusing lens and these measurements were done for ablation in vacuum (P < 5 mtorr). All holes were drilled using circular polarization and a spot size of 600 μm, and the exposure time (or number of shots) was varied (12,000 in steel and 3,000 in copper and aluminum) in order to keep the hole depths nominally near 200 μm. Fig. 5(a) shows the rate at which the main hole is drilled as a function of fluence. The rate is determined by measuring the distance from the original surface to the nominal plane of the flat bottom and dividing by the number of shots. The ablation rate for both aluminum and copper reach a maximum rate near 100 nm/pulse which is four and five times, respectively, that of stainless steel (20 nm/pulse). The fraction of incident energy absorbed at the surface, calculated from the

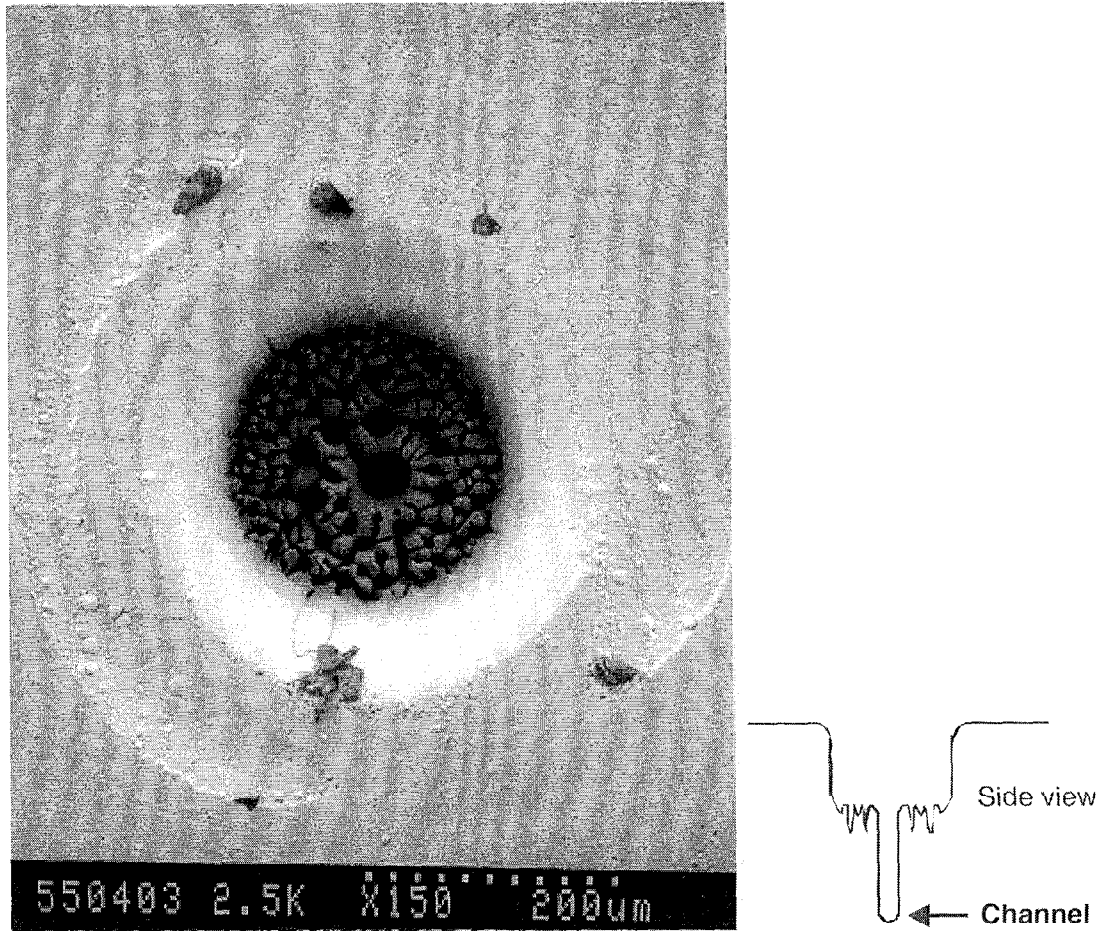


Fig. 4. SEM micrograph of hole drilled at normal incidence in stainless steel, 1 ps pulse length, circular polarization, 10 J/cm^2 . The inset is a rough depiction of how the cross-section would look.

Fresnel formulas, is .13, .04, and .39 for aluminum, copper, and steel, respectively. It does not appear that the specular reflectivity plays a significant role in determining the drilling rate of the main hole.

Most striking is the fact that from 1 to 15 J/cm^2 , the rate is independent of fluence for all of the metals although copper does not reach its saturated value until $3\text{--}4 \text{ J/cm}^2$. For aluminum, the saturated rate is reached by 1 J/cm^2 , and for stainless steel this occurs at approximately $.5 \text{ J/cm}^2$. Preuss et al.¹ report a drilling rate for copper, measured in a similar fashion, of 25 nm/pulse at 1 J/cm^2 which is below the value we measured. In addition, the logarithmic dependence on fluence predicted by the model they proposed is not evident for any of the metals reported here. Instead, for all three metals, we observed a fast rise followed by no evidence of further increase in rate with increasing fluence. This saturated behavior is further confirmed by fact that the hole bottom formed even when using a gaussian spatial profile is remarkably flat, neglecting the roughness created by the presence of channels shown in Fig. 4. This is true for all depths we have examined to this point, ranging from $100 \mu\text{m}$ to near 1 mm . Even a small difference in rate would result a measurable surface variation after tens of thousands of shots; this is not the case. It is not currently known what is causing this strong saturation of drilling rate with fluence.

Although the rate at which the hole bottom is drilled becomes essentially independent of fluence, other features develop in the hole bottom at higher fluences such as those shown in Fig. 4. The scale lengths and overall distribution of these features are very repeatable and do not correspond to any observable intensity variations in the laser spatial profile. Also, since, as mentioned above, the drilling rate for the main hole is independent of fluence, there is no reason *a priori* to expect that small intensity variation would have much of an effect. However, as the incident fluence increases, the roughness of the hole bottom also increases until at a certain threshold fluence, the distinct, circular channel forms near the location of the peak fluence. This threshold fluence is approximately 5 J/cm^2 for aluminum and stainless steel and 10 J/cm^2 for copper. The

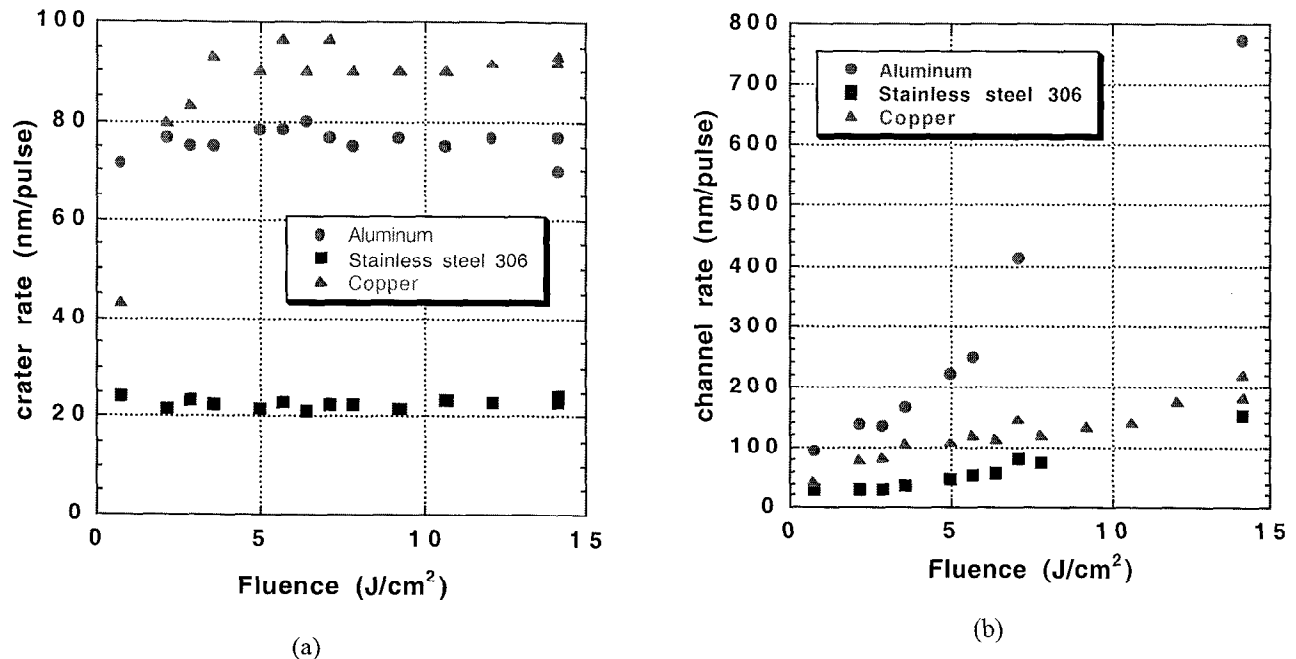


Fig. 5. (a) Ablation rate measured using depth of flat hole bottom for aluminum, stainless steel 306, and copper. (b) Ablation rate measured using depth of deepest channel in the same materials.

increase in the threshold for copper may be related to the much lower absorption for copper, although if this were the only effect, the threshold for this channel formation for aluminum should be between steel and copper. The average drilling rate of this central channel, measured by dividing the depth of the channel by the total number of pulses, is shown in Fig. 5(b) for all three metals. Here, there is no evidence of any type of saturation effects. The channel drilling rate for copper only increases by a factor of two while the rate for both stainless steel and aluminum increases by a factor of eight although this could be simply an effect of the increased channel formation threshold in copper. It should also be noted that these channels can extend several millimeters into the material, giving aspect ratios of 20:1 or higher. By comparison, Nolte et al.¹⁴ report a change in the slope of the ablation rate in copper at .5 J/cm^2 when measured using the average depth of the hole bottom. This is significantly different from the 3–4 J/cm^2 where we observe the onset of channel formation. They also report a logarithmic dependence of rate on fluence above this value which we also do not observe. Their measurements were done for a limited number of shots (10–30 μm hole depths), and the behavior we observe may not become important until the holes are deeper. The fact that they use an average depth to determine rate may also play a role.

We currently do not have an explanation of the mechanism which generates these channels for short pulse laser drilling. Our models and experiment indicate that in the fluence regime where these channels begin to form, only a few tens of nanometers are removed per pulse. This means that there must be some collective effect which is self-organizing and constructively feeds back on itself over thousands of shots. Similar features have also been observed when cutting slots by rastering the beam back and forth across the workpiece so that the beam is not incident on the same region from one pulse to the next. A series of the channels will form with quasi-periodic spacing along the length of the cut.

5. CONCLUSION

Laser materials processing using ultrashort laser pulses is capable of producing high-precision, high-quality features in a wide variety of materials from transparent dielectrics to metals to composites. The plasma plume created during ablation can also be used for diagnostics or as a source for thin film deposition. As ultrafast laser technology becomes more mature and “user-friendly,” the use of this technology in industrial settings will become more widespread.

ACKNOWLEDGEMENTS

This work was performed under the auspices of the US Department of Energy by Lawrence Livermore National Laboratory under contract No. W-7405-ENG-48.

REFERENCES

1. S. Preuss, A. Demchuk, and M. Stuke, "Sub-picosecond UV laser ablation of metals," *Appl. Phys. A* **61**, pp. 33–37, 1995.
2. B.N. Chichkov, C. Momma, S. Nolte, F. von Alvensleben, and A. Tünnermann, "Femtosecond, picosecond and nanosecond laser ablation of solids," *Appl. Phys. A* **63**, pp. 109–115, 1996.
3. P. S. Banks, B. C. Stuart, M. D. Perry, M. D. Feit, A. M. Rubenchik, J. P. Armstrong, H. Nguyen, F. Roeske, R. S. Lee, B. R. Myers, and J. A. Sefcik, in *Conference on Lasers and Electro-Optics*, Vol. 6 of Technical Digest Series (Optical Society of America, Washington, D. C., 1998), paper CFD2.
4. M. D. Perry, B. C. Stuart, P. S. Banks, M. D. Feit, V. Yanovsky, and A. M. Rubenchik, "Ultrashort-pulse laser machining of dielectric materials," *J. Appl. Phys.* **85**, pp. 6803–6810, 1999.
5. D. Ashkenasi, A. Rosenfeld, H. Varel, M. Wähler, and E. E. B. Campbell, "Laser processing of sapphire with picosecond and sub-picosecond pulses," *Appl. Surf. Sci.* **120**, pp. 65–80, 1997.
6. M. Lenzner, J. Krüger, W. Kautek, and F. Krausz, "Precision laser ablation of dielectrics in the 10-fs regime," *Appl. Phys. A* **68**, pp. 369–371, 1999.
7. T. Her, R. J. Finlay, C. Wu, S. Deliwala, and E. Mazur, "Microstructuring of silicon with femtosecond laser pulses," *Appl. Phys. Lett.* **73**, pp. 1673–1675, 1998.
8. B. C. Stuart, M. D. Feit, S. Herman, A. M. Rubenchik, B. W. Shore, and M. D. Perry, "Nanosecond-to-femtosecond laser-induced breakdown in dielectrics," *Phys. Rev. B* **53**, pp. 1749–1761, 1996.
9. B.-M. Kim, M.D. Feit, A.M. Rubenchik, B.M. Mammimi, L.B. Da Silva, "Optical feedback signal for ultrashort laser pulse ablation of tissue," *Appl. Surf. Sci.* **127-129**, pp. 857–862, 1998.
10. D. H. Lowndes, V. I. Merkulov, A. A. Puretzky, D. B. Geohegan, G. E. Jellison, Jr., G. M. Rouleau, and T. Thundat, "Amorphous diamond films deposited by pulsed laser ablation: the optimum carbon-ion kinetic energy and effects of laser wavelength," in *Advances in Laser Ablation of Materials*, v. **526**, pp. 325–330 (Materials Research Society, Warrendale, PA 1998).
11. P. S. Banks, L. Dinh, B. C. Stuart, M. D. Feit, A. M. Komashko, A. M. Rubenchik, M. D. Perry, W. McLean, "Short-pulse laser deposition of diamond-like carbon thin films," *Appl Phys A* **69**, pp. S347–S353, 1999.
12. A. M. Rubenchik, M. D. Feit, M. D. Perry, and J. T. Larson, "Numerical simulation of ultra-short laser pulse energy deposition and bulk transport for material processing," *Appl. Surf. Sci.* **127–129**, pp. 193–198, 1998.
13. A. M. Komashko, M. D. Feit, A. M. Rubenchik, M. D. Perry, P. S. Banks, "Simulation of material removal efficiency with ultrashort laser pulses," *Appl Phys A* **69**, pp. S95–S98, 1999.
14. S. Nolte, C. Momma, H. Jacobs, A. Tünnerman, B. N. Chichkov, B. Wellegehausen, and H. Welling, "Ablation of metals by ultrashort laser pulses," *J. Opt. Soc. Am. B* **14**, pp. 2716–2722, 1997.
15. P. S. Banks, M. D. Feit, A. M. Rubenchik, B. C. Stuart, and M. D. Perry, "Material effects in ultra-short pulse laser drilling of metals," *Appl. Phys. A* **69**, pp. S377–S380, 1999.